

# Information Recovery In Behavioral Networks

Tiziano Squartini,<sup>1</sup> Enrico Ser-Giacomi,<sup>2</sup> Diego Garlaschelli,<sup>3</sup> and George Judge<sup>4</sup>

<sup>1</sup>*Istituto dei Sistemi Complessi, Università di Roma ‘Sapienza’, P.le A. Moro 5, 00185 Rome (Italy)*

<sup>2</sup>*Instituto de Física Interdisciplinar y Sistemas Complejos,*

*Universitat des les Illes Balears, E-07122 Palma de Mallorca (Spain)*

<sup>3</sup>*Lorentz Institute for Theoretical Physics, University of Leiden, Niels Bohrweg 2, 2506 Leiden (Netherlands)*

<sup>4</sup>*Graduate School and Giannini Foundation, University of California Berkeley, Berkeley, CA 94720 (United States)*

(Dated: November 18, 2021)

In the context of agent based modeling and network theory, we focus on the problem of recovering micro behavior-related choice information from aggregate origin-destination data. As a basis for predicting agents' choices we emphasize the connection between adaptive intelligent behavior, causal entropy maximization and self-organized, equilibrium-seeking behavior in a dynamic system. We cast this problem in the form of a binary network and suggest information theoretic, entropy-driven methods to recover estimates of the unknown parameters connecting the behavioral data. Our objective is to recover the unknown behavioral binary parameters analytically, without explicitly sampling the configuration space. In order to do so, we enlarge the set of estimators commonly employed to make optimal use of the available information. More specifically, we consider the Cressie-Read family of entropic functionals and focus on three cases of particular interest. We then apply this information theoretic method to the analysis of both univariate and bivariate data sets.

PACS numbers: 89.75.Da; 02.50.Le; 89.65.Ef

## I. INTRODUCTION

Inference concerning behavioral choices is a central problem for socio-economic disciplines. The dynamics of social and economic systems, in fact, involves a myriad of interdependent micro-components, giving rise to a world characterized by a (nearly instantaneous) feedback-adaptive behavior that is somewhat parallel to a thermodynamic system obeying the principles of out-of-equilibrium statistical mechanics.

This implies that the socio-economic data involve dynamic, adaptive behavior systems whose evolution does not obey deterministic rules. Rather, such systems follow optimization rules driving them toward a certain, optimal stationary state associated with a functional and hierarchical structure [1–3]. This point of view differs substantially from the one adopted by current econometric and statistical analyses that rest on reductionist functional models and implies the adoption of notions as information theory, non-linearity and uncertainty.

An insightful connection between causal adaptive behavior and entropy maximization has been recently shown [4], suggesting that entropy maximization can indeed represent the general status measure/optimizing criterion in many systems. This framework permits the interpretation of adaptive socio-economic behavior in entropic terms, thus allowing one to make use of information theoretic methods. As a consequence, this consistency of the nature of *a*) socio-economic data and *b*) the information theoretic-based inference processes has the potential for turning the descriptive character of social and economic disciplines into a more quantitative one, rooted in adaptive behavior and causal entropy maximization. Remarkably, this possibility presents another advantage as it circumvents the ill-posed nature of inverse econometric problems.

In this new context, socio-economic systems are stationary state seeking but may not be in equilibrium: in fact, although there is only one stationary state consistent with an economic system in equilibrium, there is a large number of ways an economic path-dependent system may be out of equilibrium. Thus, in the behavioral area (causal) entropy maximization leads us to believe that an economic system with a large number of agents, interacting locally and in finite time, is in fact optimizing itself [2]. In this behavior-related setting, concepts such as information, commodities, economic values, optimal resource allocation and causal path entropy represent essentially the same thing.

Moreover, in the behavioral sciences everything seems to depend on everything else and this fits right into the interconnectedness/simultaneity of the non-linear, dynamic network paradigm, making this approach attractive for information recovery in the socio-economic sciences [5–8]. As an example, the representation of a market as a network comes naturally from microeconomic theory [9–11] which considers a market as a member of a microcanonical ensemble. Entropy reflects the number of ways a macrostate can evolve along a path of possible microstates: the more diverse the number of microstates, the larger the causal path entropy. The result is a causal entropic force describing the self-organized, equilibrium-seeking behavior [4, 12]. The same line of reasoning has recently led two of us to explicitly identify in equilibrium and out of equilibrium instances of economic and financial networks [13, 14].

In the sections ahead we recast the problem of recovering micro behavior-related choice information in terms of path-microstates. The specific systems we focus on for this analysis concern origin-destination networks, that constitute an important subset of observed networks and thus backbone of many dynamical processes observed in everyday life.

## II. GENERAL SETUP OF THE PROBLEM

In a behavioral network the efficiency of information flow is predicated on discovering, or designing, protocols that efficiently route information. In many ways this is like a scale-free transportation network where the emphasis is on design and efficiency in routing the traffic flows [15].

In this context, consider the problem of determining least-time point-to-point traffic flows between sub-networks, when only aggregate origin-destinations volumes are known (see fig. 1). The research question concerns the prediction of the pattern of flows along the set of pathways, given a set of measures taken along the pathways. The unknown set of pathway-specific probabilities must be often estimated from aggregate data that may be noisy in nature and the number of unknown parameters is often much larger than the number of measured aggregate origin-destination data points. If we indicate by  $\mathbf{y}$  the  $R$ -dimensional vector of observed fluxes and by  $\mathbf{x}$  the  $C$ -dimensional vector of intermediate measures, the ‘activity’ of an origin-destination network can be summed up by writing

$$\mathbf{y} = \mathbf{Ax} \quad (\text{II.1})$$

where  $\mathbf{A}$  is an  $R \times C$  rectangular matrix, encoding the information about connections. Thus, our problem translates into estimating  $\mathbf{x}$  on the basis of the  $R$ , available, components of  $\mathbf{y}$  and the connection structure  $\mathbf{A}$ . As a result, indirect and possibly noisy observable data must be used to recover information on the unobserved and unobservable model components. This means that although the observed data are considered to be directly influenced by the values of model components, the latter are not directly observable. The relationship characterizing the effect of unobservable components on the observed data must be somehow inverted to recover information concerning the unobservable model components from the accessible observations. In other words, the analyst must use indirect noisy observations to recover information on the unobserved vector of parameters and the unobserved (and unobservable) random components.

The ill-posed nature of the problem is such that the inversion of eq. II.1 is not feasible. The number of unknowns, in fact, is greater than the number of known data, i.e.  $R < C$ . As a result, in an attempt to fix the problem, multistage seeking methods such as penalized psuedo-likelihood functions, tuning parameters and calibration methods have been suggested in the literature [16–18]. Luckily, one can resort to the methodology commonly employed for solving problems of inference on the basis of partial information [19–22]. In order to do this, the problem unknowns should be interpretable as probabilities, to be estimated on the basis of some known distribution moments. In our case, this can be easily achieved by dividing both sides of II.1 by  $x_{tot} \equiv \sum_c x_c$

$$\frac{\mathbf{y}}{x_{tot}} \equiv \mathbf{r} = \mathbf{Ap} \equiv \mathbf{A} \frac{\mathbf{x}}{x_{tot}}. \quad (\text{II.2})$$

We can then rewrite II.1 in terms of *fractions of fluxes* distributed across the  $C$  channels and interpret them as unknown probabilities. Such formulation allows us to treat  $\mathbf{r} \equiv \frac{\mathbf{y}}{x_{tot}}$  as the vector of data and  $\mathbf{p} \equiv \frac{\mathbf{x}}{x_{tot}}$  as the vector of unknowns.

Notice that this peculiar definition of probability coefficients induces a distribution on the set of pathways, that play the role of an *ensemble*. Thus, II.2 allows us to restate the problem of predicting the fluxes on origin-destination networks as a (more) general problem of statistical inference, where the unknown distribution on the pathways  $\{p_c\}_{c=1}^C$  must be determined on the basis of the partial information subject to the conditions

$$\sum_c p_c = 1 \quad (\text{II.3})$$

and

$$\sum_c p_c Q_c^\alpha = \langle Q^\alpha \rangle, \quad \alpha = 1 \dots M, \quad (\text{II.4})$$

where II.4 is nothing more than II.2, rephrased in more general terms:

$$\sum_c p_c A_{\alpha c} = r_\alpha, \quad \alpha = 1 \dots R. \quad (\text{II.5})$$

A similar problem is faced when considering bivariate probability distributions, i.e. whenever a matrix of probability coefficients (and not a simple vector),  $\mathbf{P}$ , is analyzed. Problems of this type can be formulated in much the same way as univariate ones, by writing the equation

$$\mathbf{y}' = \mathbf{x}' \mathbf{P} \quad (\text{II.6})$$

and thus mimicking II.1. As we will show, treating  $\mathbf{y}'$  and  $\mathbf{x}'$  as known vectors allows us to successfully also tackle this second type of problem.

### III. METHODS

In the previous subsections we pointed out that information theoretic, entropy-based methods represent a way to deal with socio-economic data, models and the resulting behavioral inverse problems. In this context the Cressie and Read [23, 24] (CR) family of functionals provide a basis for linking the data and the unknown (and unobservable) behavioral model parameters.

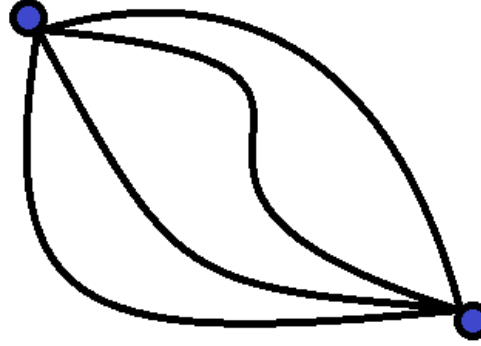


FIG. 1. A schematic representation of an origin-destination network. Blue dots represent the origin and the destination nodes. Connections between them represent the ensemble of pathways described by the probability distribution  $\{p_c\}_{c=1}^C$ . The CR family allows one to determine the probability coefficients  $p_c$ ,  $\forall c$  by making use of the available partial information, i.e. aggregate data on traffic volumes.

### A. Cressie-Read family of functionals

Solving the inference problem means choosing a functional of the probability distribution  $\{p_c\}_{c=1}^C$ , to be optimized under the constraints represented by conditions II.3 and II.4 [25, 26]. A very common choice is represented by Shannon entropy. However, the latter is only a particular case of a much more general set of divergences functionals, known as *Cressie-Read family* [27, 28]

$$I(\mathbf{p}, \mathbf{q}, \gamma) = \frac{1}{\gamma(\gamma+1)} \sum_c p_c \left[ \left( \frac{p_c}{q_c} \right)^\gamma - 1 \right] \quad (\text{III.1})$$

i.e. a family of convex, additive divergences between any two probability distributions, where  $\mathbf{p}$  is a subject distribution,  $\mathbf{q}$  is a reference-prior distribution and the parameter  $\gamma$  allows one to select among different functionals. As  $\gamma$  varies, the resulting estimator exhibits qualitatively different behavior that includes Shannon entropy, the Kullback-Leibler measure and the logistic distribution-divergence [27, 28]. In addition, the CR measure exhibits proper convexity in  $\mathbf{p}$ , for all values of  $\gamma$  and  $\mathbf{q}$ , and embodies the required probability system characteristics, such as additivity and invariance with respect to a monotonic transformation of the divergence measures. In the context of extremum metrics, the CR measures represent a flexible family of pseudo-distance measures from which to derive empirical probabilities. In what follows we consider the three values corresponding to  $\gamma = -1, 0, 1$  [29–31].

For bivariate problems, the CR family of functionals becomes

$$I(\mathbf{p}, \mathbf{q}, \gamma) = \frac{1}{\gamma(\gamma+1)} \sum_j \sum_k p_{jk} \left[ \left( \frac{p_{jk}}{q_{jk}} \right)^\gamma - 1 \right] \quad (\text{III.2})$$

subject to the conditions

$$\sum_k p_{jk} = 1, \forall j, \quad (\text{III.3})$$

$$\sum_j x'_j p_{jk} = y'_k, \forall k \quad (\text{III.4})$$

$j$  and  $k$  respectively reflecting the row and column index of the probability matrix  $\mathbf{P}$  to be estimated.

### 1. Shannon functional

In the limit as  $\gamma \rightarrow 0$

$$\lim_{\gamma \rightarrow 0} I(\mathbf{p}, \mathbf{q}, \gamma) = \sum_c p_c \ln \left( \frac{p_c}{q_c} \right) \quad (\text{III.5})$$

the *Kullback-Leibler divergence* between  $\mathbf{p}$  and  $\mathbf{q}$  is obtained. The particular case of a uniform prior,  $q_c = 1/C$ , allows us to recover the usual form of (minus) the Shannon entropy of the  $\mathbf{p}$  distribution:  $I(\mathbf{p}, \frac{1}{C}, 0) = \sum_c p_c \ln p_c + \ln C$ .

### 2. Likelihood functional

In the limit as  $\gamma \rightarrow -1$  provides the second functional of our list

$$\lim_{\gamma \rightarrow -1} I(\mathbf{p}, \mathbf{q}, \gamma) = \sum_c q_c \ln \left( \frac{q_c}{p_c} \right) \quad (\text{III.6})$$

the *Kullback-Leibler divergence* between  $\mathbf{q}$  and  $\mathbf{p}$ . The particular case of uniform prior  $q_c = 1/C$  allows us to recover the usual form of (minus) the likelihood function of the  $\mathbf{p}$  distribution:  $I(\mathbf{p}, \frac{1}{C}, -1) = -\sum_c \frac{\ln p_c}{C} - \ln C$ .

### 3. Euclidean functional

The value  $\gamma = 1$  provides the third functional

$$I(\mathbf{p}, \mathbf{q}, 1) = \sum_c \frac{p_c}{2} \left( \frac{p_c}{q_c} - 1 \right) \quad (\text{III.7})$$

which, in the particular case of uniform prior  $q_c = 1/C$ , allows us to recover the form  $I(\mathbf{p}, \frac{1}{C}, 1) = \frac{C}{2} \sum_c p_c (p_c - \frac{1}{C})$ .

## B. A statistical inference procedure

Once the functional has been chosen by tuning the parameter  $\gamma$  to the desired value, the constraints come into play defining the so-called *Lagrangean function*

$$\mathcal{L} = I(\mathbf{p}, \mathbf{q}, \gamma) - \theta_0 \left[ \sum_c p_c - 1 \right] - \sum_{\alpha} \theta_{\alpha} \left[ \sum_c p_c Q_c^{\alpha} - \langle Q^{\alpha} \rangle \right] \quad (\text{III.8})$$

i.e. the quantity to optimize in order to find the mathematical expression of our probability coefficients. In particular, since the functional  $I$  is a divergence, the Lagrangean function has to be minimized with respect to the vector of coefficients  $\mathbf{p}$ :

$$\frac{\partial \mathcal{L}}{\partial p_c} = 0, \forall c. \quad (\text{III.9})$$

The resolution of the system III.9 gives us the desired coefficients  $p_c$  as functions of the Lagrangean multipliers,  $p_c = p_c(\vec{\theta})$ . Once found, the parametric probability coefficients must be substituted back into  $\mathcal{L}$ , in order to obtain a quantity which is a function of the unknowns solely:  $\mathcal{L}(\vec{\theta})$ .

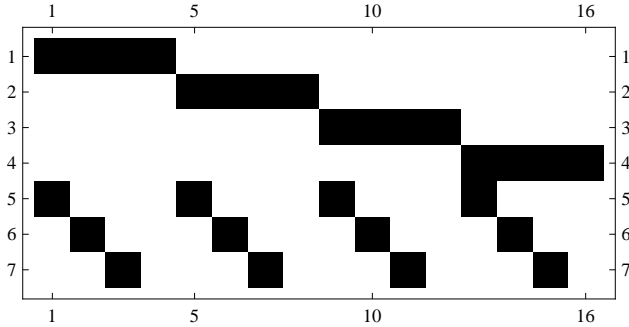


FIG. 2. Pictorial matrix representation of a local area network at Bell Labs (black squares represent ones, white dots represent zeros) [19, 32]. The network topology we consider yields 7 observed aggregate traffic volumes and 16 origin-destination traffic volumes.

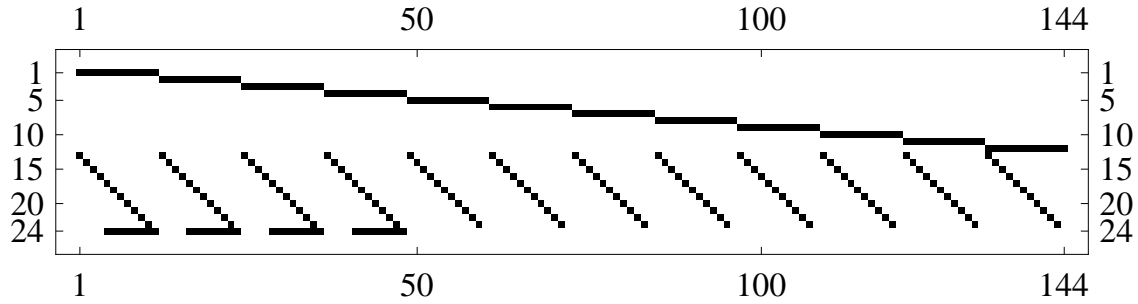


FIG. 3. Pictorial matrix representation of a local area network at the Information Networking Institute of Carnegie Mellon University (black squares represent ones, white dots represent zeros) [32]. The network topology we consider yields 24 observed aggregate traffic volumes and 144 origin-destination traffic volumes.

The last step of our procedure is the optimization of the function  $\mathcal{L}(\vec{\theta})$ ; by finding the values of the parameters  $\vec{\theta}^*$  satisfying the condition

$$\vec{\nabla} \mathcal{L} |_{\vec{\theta}^*} = 0 \quad (\text{III.10})$$

allows us to test the consistency of our procedure, by verifying that

$$\frac{\partial \mathcal{L}}{\partial \theta_0} = 0 \implies \sum_c p_c(\vec{\theta}) = 1, \quad (\text{III.11})$$

$$\frac{\partial \mathcal{L}}{\partial \theta_\alpha} = 0 \implies \sum_c p_c(\vec{\theta}) Q_c^\alpha = \langle Q^\alpha \rangle. \quad (\text{III.12})$$

The vector  $\vec{\theta}^*$  allows us to numerically evaluate the probability coefficients, which are indicated by  $p_c^* \equiv p_c(\vec{\theta}^*)$ ,  $\forall c$ . The latter permits us to produce the estimate  $\mathbf{x}^* = \mathbf{p}^* x_{tot}$  to be compared with the real, observed  $\mathbf{x}$ . Naturally,  $\mathbf{r}^* = \mathbf{A} \mathbf{p}^* = \mathbf{r}$ .

For bivariate problems, the number of multipliers rises, since the required number of normalization conditions is equal to the number of matrix rows. Thus, in order to correctly implement our approach, two vectors  $\vec{\alpha}$  and  $\vec{\beta}$  must be considered (see the Appendix).

#### IV. DATA

To test the effectiveness of our method, in what follows we will analyze two aggregate traffic data sets (for which origin-destination traffic volumes were collected) and two bivariate networks.

TABLE I. Observed bivariate distribution of the number of times bacon and eggs were purchased on four consecutive shopping trips [20, 33].

Bacon	Eggs					Total
	0	1	2	3	4	
0	254	115	42	13	6	430
1	34	29	16	6	1	86
2	8	8	3	3	1	23
3	0	0	4	1	1	6
4	1	1	1	0	0	3
Total	297	153	66	23	9	548

TABLE II. Precinct-level data of Louisiana's 5th CD elections [20].

	Rep.	Dem.	Ind.1	Ind.2	Abst.	Total
White	—	—	—	—	—	1158
Black	—	—	—	—	—	222
Other	—	—	—	—	—	31
Total	963	207	28	17	196	1411

### A. Bell Labs data

The first data set involves traffic volumes on a local area network at Bell Labs [19, 32]. The network topology we consider yields 7 observed aggregate traffic volumes and 16 origin-destination traffic volumes. Aggregate volumes were measured every five minutes, over one day, on the Bell Labs corporate network. This implies a set of measurements at 287 points in time (see fig. 2).

### B. Carnegie University data

The second dataset was collected at the Information Networking Institute of Carnegie Mellon University [32]. The network topology we consider yields 24 observed aggregate traffic volumes and 144 origin-destination traffic volumes (see fig. 3), observed every five minutes (473 points in time). This second dataset is larger than the first, allowing us to test the scalability of our approach.

### C. Bivariate networks

The bivariate networks we have analyzed are described by the two datasets reported in [20, 33].

The first dataset comes from an economic case-study and relates to consumer behavior in the purchase of eggs and bacon. In particular, data consist of a sample of 548 independent households and the purchased products at the market, recorded over 4 consecutive trips. For each trip, it was recorded whether or not the household purchased eggs, bacon or both: the matrix entries represent the number of times a given customer purchased bacon and eggs over the course of the 4 trips (see table I) [33].

The second dataset comes from an application in political science and concerns voter behavior and candidate choice (see table II) [20].

## V. RESULTS

In the following subsections we describe the results we obtained by applying our procedure to the study of the aforementioned four datasets.

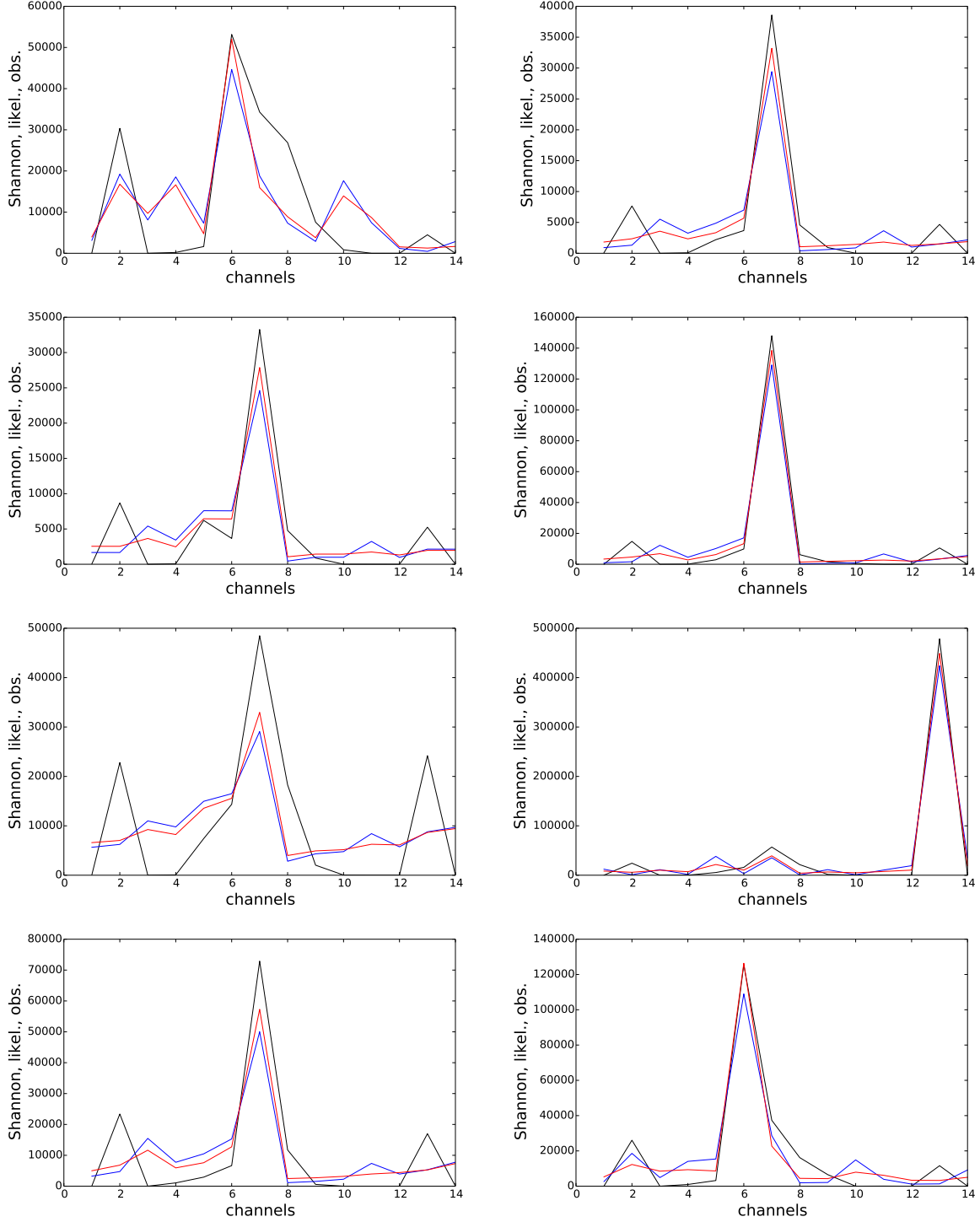


FIG. 4. Analysis of Bell Labs data corresponding to ten chosen time points. The number of the channel is reported on the x-axis. Our estimations of  $x$  are reported on the y-axis. Colors refers to: observed data (black trend), our estimation based on Shannon functional (blue trend), our estimation based on the likelihood functional (red trend).

### A. Bell Labs data

The analysis of Bell Labs data is illustrated in figs. 4, 5. The panels report what we have called ‘channel plot’, showing the number of the origin-destination pattern on the x-axis and the traffic volume mea-

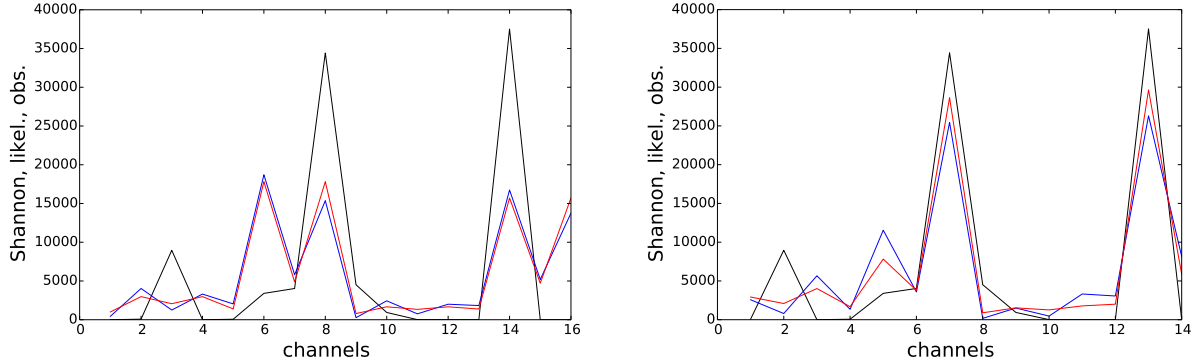


FIG. 5. Analysis of Bell Labs data for the 90th time point. The number of the channel is reported on the x-axis. Our estimations of  $\mathbf{x}$  are reported on the y-axis. Colors refer to: observed data (black trend), our estimation based on Shannon functional (blue trend), our estimation based on the likelihood functional (red trend). Left panel: zero traffic flows are included in the data set. Right panel: zero traffic flows are excluded from the data set.

sured/estimated on it, on the y-axis. Black trends represent the observed traffic volumes and colored trends represent the expected traffic volumes, predicted via our procedure: blue trends represent the prediction obtained with Shannon functional, red trends represent the prediction obtained with the likelihood functional. Each panel corresponds to a given time point, chosen among the 287 available ones.

As a general comment, both the predictions reproduce the majority of the observed trends satisfactorily, with the likelihood functional performing slightly better than Shannon functional whose estimates, in some cases, show larger discrepancies. Moreover, the performance of both functionals improves when single peaks are registered on a single channel, accompanied by small traffic volumes on the others. However, whenever the latter are exactly zero the agreement between our estimates and observations seems to deteriorate: as shown in the left panel of fig. 5, if zero traffic flows happen to be measured on some line (in this case, the 1st and the 16th for the 90th temporal measurement), both Shannon and the likelihood functionals predict smaller peaks and larger values for the neighboring lines.

A solution to improve the predictions accuracy is to explicitly exclude zero values from our dataset. This can be achieved by considering a reduced  $\mathbf{x}$  vector and a reduced  $\mathbf{A}$  matrix without the 1st and the 16th columns, i.e. precisely those contributing to the values  $x_1 = x_{16} = 0$ . The right panel of fig. 5 shows the improved accuracy of our method: notice how peaks are reproduced much better now and traffic values on the neighboring lines are predicted to be much smaller than the former, as observed values confirm. The predicted trends in fig. 4 are calculated by adopting the same criterion, i.e. explicitly excluding the zero values on the extreme channels.

The Euclidean functional (not shown in figs. 4, 5) performs worst: its functional form often leads to problems of numerical convergence and, in any case, is characterized by the largest discrepancies between expected and observed patterns.

## B. Carnegie University data

The analysis of Carnegie University data is illustrated in fig. 6. Generally speaking, our method captures again the chosen temporal trends, implying that our procedure is scalable, i.e. applicable to problems with higher dimensionality. However, the results concerning Carnegie University data present some differences with respect to the Bell Labs ones.

Since a visual inspection of fig. 6 is not feasible, to quantify the agreement between our estimates and the observations we have calculated the Pearson correlation coefficient between the observed trends and each of the expected ones. The results for the Shannon functional are:  $r = 0.994$  for the upper left panel (1st time point),  $r = 0.991$  for the upper right panel (3rd time point),  $r = 0.996$  for the middle left panel (80th time point),  $r = 0.985$  for the middle right panel (190th time point),  $r = 0.989$  for the bottom left panel (330th time point) and  $r = 0.993$  for the bottom right panel (456th time point). The results for the likelihood functional are (in the same order):  $r = 0.581$  (1st time point),  $r = 0.595$  (3rd time point),  $r = 0.703$  (80th time point),  $r = 0.699$  (190th time point),  $r = 0.693$  (330th time point) and  $r = 0.701$  (456th time point).

Despite the rather high values of  $r$ , the strongly oscillatory character of the observed data set seems to

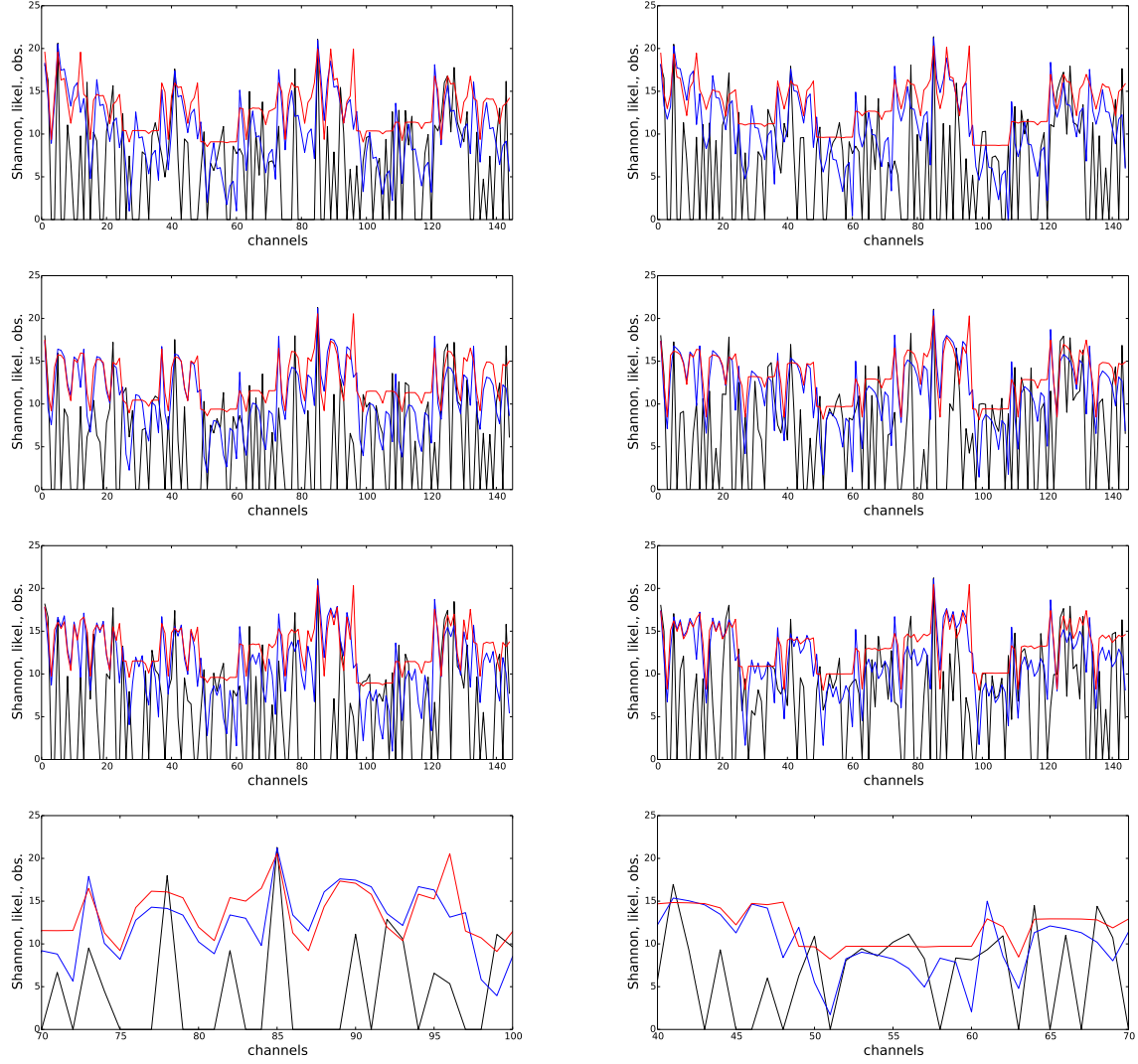


FIG. 6. Analysis of Carnegie University data corresponding to six chosen time points. The number of the channel is reported on the x-axis. Our estimations of  $x$  are reported on the y-axis (logarithmic scale). Colors refer to: observed data (black trend), our estimation based on Shannon functional (blue trend), our estimation based on the likelihood functional (red trend). The lowest panels show a zoomed region of the ‘channel plots’ corresponding to the 80th and 190th time points.

have the effect of lowering the performance of our procedure: in fact, our estimations predict a ‘smoother’ behavior than that of real data which, on the other hand, appear much more irregular (see lower panels of fig. 6). As for the Bell Labs data set, the net result is that high values of traffic data are well estimated while the lower ones (included the zero ones) are generally overestimated.

Quite surprisingly, even the differences characterizing the performances of the two functionals are larger than those for the Bell Labs data set: this time the best result (witnessed by the higher Pearson coefficients for all the time points) is obtained by the Shannon functional which seems to better follow the irregular observed trends: the predictions obtained by the likelihood functional, in fact, show flat regions which in turn have the effect of lowering the numerical value of  $r$ .

### C. Bivariate networks

The result of the application of our method to the ‘eggs and bacon’ data set is shown in table III. Being a bivariate network, the predictions of our functionals concern the matrix entries, estimated from the available

TABLE III. Expected bivariate distribution of the number of times bacon and eggs were purchased on four consecutive shopping trips [20, 33].

		Shannon functional						
Bacon	0	Eggs						
		1	2	3	4			
0	262.378	122.478	40.468	4.65702	0.0191661	0.999453		
1	27.3702	23.502	18.8328	12.2212	4.0738	0.970398		
2	5.38417	5.16918	4.87188	4.33981	3.23497	0.86233		
3	1.25404	1.24078	1.22175	1.18545	1.09798	-0.0718339		
4	0.613532	0.61028	0.605583	0.596516	0.574089	0.847078		
		Likelihood functional						
Bacon		Eggs						
0	1	2	3	4				
0	258.603	118.489	40.1875	9.81096	2.90897	0.99991		
1	30.4192	26.7046	18.5562	7.63744	2.68261	0.993516		
2	6.02486	5.86333	5.34772	3.78732	1.97677	0.850168		
3	1.32087	1.31294	1.28519	1.1694	0.911598	0.019223		
4	0.631723	0.629903	0.623446	0.594872	0.520056	0.824691		
		Euclidean functional						
Bacon		Eggs						
0	1	2	3	4				
0	265.873	127.823	44.4184	3.19533	14.916	0.997586		
1	24.1851	18.6631	15.3269	13.678	14.1468	0.908502		
2	5.09961	4.70465	4.46603	4.34809	4.38162	0.863061		
3	1.234	1.20712	1.19088	1.18286	1.18514	-0.490478		
4	0.6085	0.60178	0.597721	0.595714	0.596285	0.687752		

rows and columns totals.

Table III depicts the predictions based on Shannon functional, the likelihood functional and the Euclidean functional. In order to further condense the information, we have also calculated the Pearson correlation coefficient between each observed row and the corresponding expected one, reporting the obtained values in the last entry of each row of table III. The correlation coefficients are high for all the three functionals, which predict very similar values to the observed ones.

A closer inspection of table III reveals that the worst agreement is obtained precisely for the entries filling the last two rows of table I, i.e. for the rows with the presence of zeros. This seems to confirm the difficulties in handling zero values met in the analysis of the Bell Labs and Carnegie University data sets: for example, Shannon functional tends to predict similar values for all entries of the last two rows (see the first sub-table). As for the Bell Labs data set, the likelihood functional performs better than Shannon one (see the second sub-table): the predicted entries are closer to the real ones and the Pearson correlation coefficients are higher; however, the rows with the zeros are still poorly reproduced. The Euclidean functional is still the one performing worst: the correlation coefficients corresponding to the last two rows of the third sub-table are the lowest.

The result of the application of our method to the elections percentages is shown in table IV. Since, because of privacy issues, the percentage of people voting for a given candidate is not available, the second bivariate data set we analyzed provides only aggregate data about the elections results and thus the single matrix entries are missing. Nonetheless, our method provides a prediction of the unknown entries, by adopting the same procedure used for the ‘eggs and bacon’ problem. As can be seen from table IV, Shannon functional and the likelihood functional give very similar estimates of the voting percentages: this similarity is effectively summed up by the ‘global’ Pearson correlation coefficient between the Shannon expected matrix and the likelihood expected matrix (both treated as an unique vector of numbers): 0.988716. It should be noted, however, that significative differences can be observed for the percentages referring to the independent candidates. Nonetheless, if interpreted in the light of the previous results, these differences carry an important information, signalling that independent candidates true percentages are not only (probably) the lowest ones,

TABLE IV. Estimated precinct-level percentages of Louisiana's 5th CD elections [20].

		Shannon functional							
		Rep.	Dem.	Ind.1	Ind.2	Abst.	Total		
White	877.555	144.824		0.968424	0.0422665	134.611	1158		
Black	78.5616	55.6173		21.2953	11.6828	54.843	222		
Other	6.88327	6.55916		5.73627	5.27497	6.54634	31		
		Likelihood functional							
		Rep.	Dem.	Ind.1	Ind.2	Abst.	Total		
White	865.704	141.143		12.2831	6.89041	131.831	1158		
Black	89.4101	58.4307		10.9359	6.44502	56.7707	222		
Other	7.7549	7.41397		4.77993	3.66401	7.38656	31		
Total	963	207		28	17	196	1411		

but even compatible with zero.

As with the univariate datasets concerning the Bell Labs and the Carnegie University, the Euclidean functional (not reported in table IV) often shows convergence problems.

## VI. DISCUSSION

Socio-economic systems seem to evolve in such a way to maximize entropy: this intuition can be formalized by introducing a broad family of entropic functionals, i.e. the Cressie-Read (CR) family, to be maximized under the constraints provided by the available information. The CR family translates ill-posed inverse problems into the language of constrained entropy maximization problems: in other words, this family of functionals allows one to solve problems characterized by a number of unknowns larger than the number of known data, by formally treating them as inference problems.

The two subsequent optimization steps characterizing our procedure can be interpreted as a ‘generalized entropy’ maximization followed by a ‘generalized likelihood’ maximization, with the concept of entropy being replaced by (the more general) concept of divergence and the word likelihood indicating the parametric form of the aforementioned divergence for the case at hand. Remarkably, this procedure works for univariate as well as bivariate data sets, as the many examples of the CR family applicability provided in this work show.

Our results indicate that the performance of functionals constituting the CR family may vary significantly: in some cases, the likelihood functional (obtained by taking the limit  $\gamma \rightarrow -1$ ) provides the best performance; in others, it is outperformed by the Shannon functional (obtained by taking the limit  $\gamma \rightarrow 0$ ). This indicates the such functionals make the best possible use of the available information, predicting the values closest to the observed ones (e.g. for the ‘eggs and bacon’ data set). This also indicates that, whenever the observed data are not available (as for the elections data), their predictions can still be considered the most trustworthy.

In turn, these findings suggest a possible optimization of our procedure, by implementing a convex combination of the proposed functionals in order to retain the predictive power of both. One of the possible alternatives is represented by Jeffreys’ entropy [34], i.e. the combination of Shannon entropy and the likelihood functional, with coefficients 1/2:

$$I_{1/2}(\mathbf{p}, \mathbf{q}) \equiv \frac{1}{2}I(\mathbf{p}, \mathbf{q}, 0) + \frac{1}{2}I(\mathbf{p}, \mathbf{q}, -1). \quad (\text{VI.1})$$

On the other hand, both the likelihood and the Shannon functionals seem to show some limitations whenever zero entries are encountered in data: however, explicitly excluding the latter (such as night time flows) from the data set, whenever feasible, greatly improves the performance of the considered pair of functionals.

Remarkably, our procedure can be further generalized in many other ways. A first example concerns the choice of the prior distribution  $\mathbf{q}$ , which could be chosen to be different from the uniform one. For instance, by explicitly carrying on the calculations for the Euclidean functional the following term appears:

$$\sum_c q_c \sum_\alpha \lambda_\alpha A_{\alpha c} = \sum_\alpha \lambda_\alpha \sum_c q_c A_{\alpha c}; \quad (\text{VI.2})$$

now, since  $\mathbf{r} = \mathbf{Ap} = \sum_c p_c A_{\alpha c}$ , choosing a prior  $\mathbf{q}$  means giving a ‘prior’ estimate of the sums  $\mathbf{r}$ . This, in turn, represents an additional constraint to the aggregated ones, to be used to potentially improve the performance of this particular functional.

A second example concerns the choice of a methodology analogous to the Akaike Information Criterion to improve the performance of a specific functional with respect to the others. However, AIC is not feasible (as well as BIC or similar ones) since all the considered functionals are characterized by the same number of parameters, i.e. the number of constraints. An alternative choice could be represented by the squared error-quadratic loss criterion [30], to make optimal use of a given set of discrete alternatives for the CR family.

Summing up, the network-based approach we have proposed in this paper questions the use of traditional information-recovery methods as a solution basis for pure and stochastic inverse type problems [25] and represents a contribution to the study of behavioral information recovery from dynamic economic systems. Our findings open a promising perspective on ways to deepen the connections between adaptive behavior and causal entropy maximization in dynamic, self-organizing and equilibrium-seeking systems.

## VII. APPENDIX

For exposition purposes, let us explicitly demonstrate the analytical derivation of the Shannon functional for univariate datasets. Recalling equation III.5, in this case the probability coefficients have the expression

$$\frac{\partial \mathcal{L}}{\partial p_c} = 0 \implies p_c = q_c (e^{-1+\theta_0+H_c}), \forall c \quad (\text{VII.1})$$

while  $H_c \equiv \sum_\alpha \theta_\alpha Q_c^\alpha$ . Substituting the  $p_c$  back into  $\mathcal{L}$  produces a quantity solely function of the vector of unknown parameters  $\vec{\theta}$ . Deriving  $\mathcal{L}(\vec{\theta})$  with respect to  $\theta_0$  and  $\theta_\alpha$  allows us to explicitly find the two consistency conditions

$$\frac{\partial \mathcal{L}}{\partial \theta_0} = 0 \implies \sum_c q_c (e^{-1+\theta_0+H_c}) = 1, \quad (\text{VII.2})$$

$$\frac{\partial \mathcal{L}}{\partial \theta_\alpha} = 0 \implies \sum_c \left[ \frac{q_c e^{H_c}}{\sum_c q_c e^{H_c}} \right] Q_c^\alpha = \langle Q^\alpha \rangle. \quad (\text{VII.3})$$

In terms of the matrix form of the available data sets considered so far, our probability coefficients can be rewritten as

$$p_c = \frac{q_c e^{\sum_\alpha \theta_\alpha A_{\alpha c}}}{\sum_c q_c e^{\sum_\alpha \theta_\alpha A_{\alpha c}}}, \forall c \quad (\text{VII.4})$$

and the function to optimize with respect to the vector  $\vec{\theta}$  as

$$\mathcal{L}(\vec{\theta}) = -\ln \left[ \sum_c q_c (e^{\sum_\alpha \theta_\alpha A_{\alpha c}}) \right] + \sum_\alpha \theta_\alpha r_\alpha. \quad (\text{VII.5})$$

For bivariate datasets, on the other hand, constraining equation III.2 leads to

$$I \left( \mathbf{p}, \frac{1}{C}, 0 \right) = \sum_j \sum_k p_{jk} \ln p_{jk} + \ln C - \sum_j \beta_j \left( \sum_k p_{jk} - 1 \right) - \sum_k \alpha_k \left( \sum_j p_{jk} x'_j - y'_k \right) \quad (\text{VII.6})$$

and maximizing it with respect to  $p_{jk}$  implies that the functional form of our coefficients is

$$p_{jk} = \frac{e^{\alpha_k x'_j}}{\sum_k e^{\alpha_k x'_j}}, \forall j, k. \quad (\text{VII.7})$$

By substituting back the latter into  $\mathcal{L}$  we get

$$\mathcal{L}(\vec{\alpha}) = - \sum_j \ln \left[ \sum_k e^{\alpha_k x'_j} \right] + \sum_k \alpha_k x'_j \quad (\text{VII.8})$$

and similar results are obtained for the other functionals.

## ACKNOWLEDGEMENTS

TS acknowledges support from the Italian PNR project CRISIS-Lab.  
 ESG acknowledges support from the European Commission Marie-Curie ITN program (FP7-320 PEOPLE-2011-ITN) through the LINC project (no. 289447).  
 DG acknowledges support from the Dutch Econophysics Foundation (Stichting Econophysics, Leiden, the Netherlands) with funds from beneficiaries of Duyfken Trading Knowledge BV, Amsterdam, the Netherlands. This work was also supported by the EU project MULTIPLEX (contract 317532) and the Netherlands Organization for Scientific Research (NWO/OCW).

---

[1] Georgescu-Roegen, N. 1971. The Entropy law and the Economic process. Harvard University Press, Harvard.

[2] Annila, A. and Salthe, S. 2009. Economies Evolve by Energy Dispersal. *Entropy* 11:606-633.

[3] Raine, A., Foster, J. and Potts, J. 2006. The New Entropy Law and the Economic Process. *Ecological complexity* 3:354-360.

[4] Wissner-Gross, A. D. and Freer, C. E. 2013. Causal Entropic Forces. *Physical Review Letters* 110:168702.

[5] Mastrandrea, R., Squartini, T. and Garlaschelli, D. 2014. Enhanced reconstruction of weighted networks from strengths and degrees. *New Journal of Physics* 16:043022.

[6] Mastrandrea, R., Squartini, T. and Garlaschelli, D. 2014. Reconstructing the world trade multiplex: the role of intensive and extensive biases. *Physical Review E* 90:062804.

[7] Cimini, G., Squartini, T., Gabrielli A. and Garlaschelli, D. 2014. Systemic risk analysis in reconstructed economic and financial networks. <http://arxiv.org/pdf/1411.7613.pdf>.

[8] Cimini, G., Squartini, T., Gabrielli A. and Garlaschelli, D. 2014. Estimating topological properties of weighted networks from limited information. <http://arxiv.org/pdf/1409.6193.pdf>.

[9] Willinger, W., Alderson, D. and Doyle, J. 2009. Mathematics and the Internet: A Source of Enormous Confusion and Great Potential. *Journal of the American Mathematical Society* 56:586-599.

[10] Barabasi, A.-L. 2012. The Network Takeover. *Nature Physics* 8:14-16.

[11] Bargigli, L., Lionetta S. A. and Viaggiu, S. 2013. A Statistical Representation of Markets As complex Networks, <http://arxiv.org/pdf/1307.0817v1.pdf>.

[12] Hartonen, T. and Annila, A. 2012. Natural networks as thermodynamic systems. *Complexity* 18:5362.

[13] Squartini, T. and Garlaschelli, D. 2013. Economic networks in and out of equilibrium. *Proceedings of the Ninth International Conference on Signal-Image Technology & Internet-based Systems (SITIS 2013)* 530-537 (edited by IEEE), doi:10.1109/SITIS.2013.89.

[14] Squartini, T. and Garlaschelli, D. 2014. Stationarity, non-stationarity and early warning signals of economic networks. *Journal of Complex Networks*, doi:10.1093/comnet/cnu012.

[15] Castro, R., Coates, M., Laing, G., Nowak, R. and Yu, B. 2004. Network Tomography: Recent Developments. *Statistical Science* 19:499-517.

[16] Tibshirani, R. 1996. Regression Shrinkage and Selection Via The Lasso. *Journal of the Royal Statistical Society, B* 58(1):267-288.

[17] Hastie, T., Tibshirani, R. and Trevor, J. 2009. The Elements of Statistical learning. Springer-Verlag, New York.

[18] Smith, A., Bernheim, D., Camerer, C. and Rangel, A. 2014. Neural Activity Reveals Preferences Without Choices. *American Economic Journal: Microeconomics* 6(2):1-36.

[19] Cho, W. and Judge, G. 2014. An information theoretic approach to network tomography. *Applied Economics Letters*, doi:10.1080/13504851.2013.866199.

- [20] Cho, W. and Judge, G. 2006. Information Theoretic Solutions for Correlated Bivariate Processes. *Economic Letters* 7:201-207.
- [21] Ziebart, B., Bagnell, J. and Dey, A. 2010. *Proceedings of an International Conference on Machine Learning* (Hiafa, Israel).
- [22] Ziebart, B., Bagnell, J. and Dey, A. 2013. The principle of Maximum Causal Entropy for Estimating Interacting Processes. *IEEE Transactions For Information Theory* (in press).
- [23] Cressie, N. A. and Read, T. 1984. Multinomial Goodness of Fit Tests. *Journal of the Royal Statistical Society, B* 46:440-464.
- [24] Read, T. and Cressie, N. A. 1988. Goodness of Fit Statistics for Discrete Multivariate Data. Springer-Verlag, New York.
- [25] Pressé, S., Ghosh, K., Lee, J. and Dill, K. 2013. Principles of Maximum Entropy and Maximum Caliber in Statistical Physics. *Reviews of Modern Physics* 85:1115-1141.
- [26] Squartini, T. and Garlaschelli, D. 2011. Analytical maximum-likelihood method to detect patterns in real networks. *New Journal of Physics* 13:083001.
- [27] Gorban, A. N. and Karlin, I. V. 2003. Family of Additive Entropy Functions out of Thermodynamic Limit. *Physical Review E* 67:016104.
- [28] Gorban, A., Gorban, P. and Judge, G. 2010. Entropy: The Markov Ordering Approach. *Entropy* 12:1145-1193.
- [29] Judge, G. and Mittelhammer, R. C. 2012. An Information Theoretic Approach To Econometrics. Cambridge University Press, Cambridge.
- [30] Judge, G. and Mittelhammer, R. C. 2012. Implications of the Cressie-Read Family of Additive Divergences for Information Recovery. *Entropy* 14:2427-2438.
- [31] Mittelhammer, R. and Judge, G. 2011. A family of empirical likelihood functions and estimators for the binary response model. *Journal of Econometrics* 164:207-217.
- [32] Airoldi, E. M. and Blocker, A. W. 2013. Estimating latent processes on a network from indirect measurements. *Journal of the American Statistical Association* 108(501):149-164.
- [33] Crackel, R. and Flegal, J. M. 2014. Approximate Bayesian computation for a flexible class of bivariate beta distributions. <http://arxiv.org/pdf/1402.1782.pdf>.
- [34] Jeffreys, H. 1983. Theory of Probability. Clarendon Press, Oxford.